High power PCB-embedded inductors based on ferrite powder

Rémy CAILLAUD[1,2], Cyril BUTTAY[2], Johan LE LESLE[1,3], Florent MOREL[3], Roberto MRAD[1], Nicolas DEGRENNE[1], Stefan MOLLOV[1], Céline COMBETTES[4]

[1]Mitsubishi Electric
Research Centre Europe
1, allée de Beaulieu CS 10806
35708 RENNES CEDEX 7
France

[2]Université de Lyon
CNRS, UMR5005
INSA-Lyon
Laboratoire Ampère,
21 avenue Capelle
F-69621, France
cyril.buttay@insa-lyon.fr

[3]Université de Lyon
CNRS, UMR5005
École Centrale de Lyon
Laboratoire Ampère,
36, avenue Guy de Collongue
F-69134, France

[4]Université de Toulouse;
UPS, INPT; LAPLACE;
118 rte de Narbonne - Bât. 3R3
CNRS; LAPLACE;
F-31062 Toulouse, France

Abstract

Inductors used in power converters are usually large and complex to manufacture. As a consequence, it is desirable to integrate them within printed circuit boards, to use an otherwise wasted volume. Solid magnetic cores are brittle, and can be damaged during the PCB manufacturing (lamination). In this paper, we present a process based on ferrite powder instead of a solid core. Process details and electrical measurement results are given. Magnetic cores of up to 50 mm in diameter are produced. Magnetic permeability of up to 28 are achieved, using some MnZn ferrite powder. A final discussion summarises the advantages and disadvantages of this technique.

Keywords

PCB, power electronics, manufacturing process, characterisation

1 Introduction

With the ever-reducing size of electronic systems, it becomes desirable to embed some components within the printed circuit boards (PCBs) themselves. A review of embedding technologies is given in [1]. At the moment, a large effort has been dedicated to embedding low-power components (logic ICs, low voltages capacitors, resistors).

When considering power electronics, most of the research teams focus on integrating power semiconductor dies [2]. This is because die embedding offers improved thermal management (shorter path from the die to the heatsink) and lower parasitic inductance. Power passive components (capacitors and inductors) tend to be large, because they are used for energy storage. This makes them more complicated to embed.

However, there still are some incentives towards the embedding of passive components: although their dissipated power density is usually much lower than that of semiconductor dies, cooling is still an issue with passive components, so an improved thermal management is desirable. Also, the thickness of the PCB is often an unused space. Placing as many components (active as well as passive) as possible in this space is a net volume gain. Finally, some passives, especially the magnetic components, require a dedicated manufacturing process (custom design, assembly, winding…). Embedding them in the PCB means that all these components are built at the same time (batch process), with few added process steps.

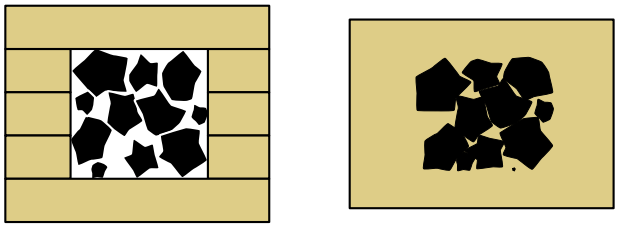

Figure 1: Embedding of ferrite powder. (a): the ferrite powder is placed in a mould formed by stacked prepreg layers. (b) during lamination under pressure, the resin contained in the prepreg flows and infiltrates the powder, forming a single, cured part.

A direct approach for the embedding of magnetic components is to use solid cores [4–7]. As they are brittle, special care must be given so that the cores are not damaged during the PCB lamination. In [5], the authors select a flat core shape, as it can withstand pressure. In [7], a gap is introduced between both parts of the core to introduce some compliance.

Another approach is to use more compliant magnetic materials. A first solution to improve mechanical com-

Manufacturing work-flow

a prepreg sheets are cut using a CO_2 laser (Gravograph). A high glass transition temperature material (Isola PCL370 HR 1080, T_g=180 °C) is used. Thin bridges are formed to keep the centre of the tore attached to the sheet.

b a release film (Pacolon HT2000), a copper foil, and the prepreg sheets are stacked on a metal platen, using registration pins for alignment.

c this first stack is pressed at low temperature (70 °C, 20 bar), to achieve light bonding between the prepreg sheets, without actually curing the resin. This bond is sufficient to prevent the ferrite powder to infiltrate between the prepreg sheets, and to maintain the centre of the core once the bridges are cut.

d the top platen is removed. The prepregs are now lightly bonded together;

e The bridges are cut using a sharp knife (cutting is easy, as the resin remain un-cured). A photograph is shown in Fig. 3.

f the ferrite powder (FMS 0.250, [3]) is poured in the cavity. The back of the metal platen is gently tapped to form a uniform ferrite layer. Any material excess is trimmed with a metal squeegee. The surface of the prepreg is cleaned of ferrite particles with a small brush.

g the stack is completed with a plain prepreg sheet, a second copper foil and releasing film. A second metal platen is placed on top, and the stack is placed in a heating press (Specac Atlas), for the final laminating cycle: a heating ramp (6 °C/mn up to 195 °C), and a 90 mn step at 195 °C. Laminating pressure is 10 bar at the beginning of the process, and is then increased up to 20 bar once the temperature exceeds 100 °C. During this final lamination step, the resin becomes liquid, and is expected to infiltrate between the ferrite particles. Once cooled down, the stack now forms a solid, coherent part.

h Holes are drilled in the PCB laminate, in preparation for the winding formation, using a CNC drill (Bungard CCD/2/ATC).

i The holes are plated with copper, using regular PCB chemistry (Bungard, using a Compacta plating station, also from Bungard), and the copper layers are selectively masked with a photosensitive dry film (Dupont Riston) and patterned with ferric chloride.

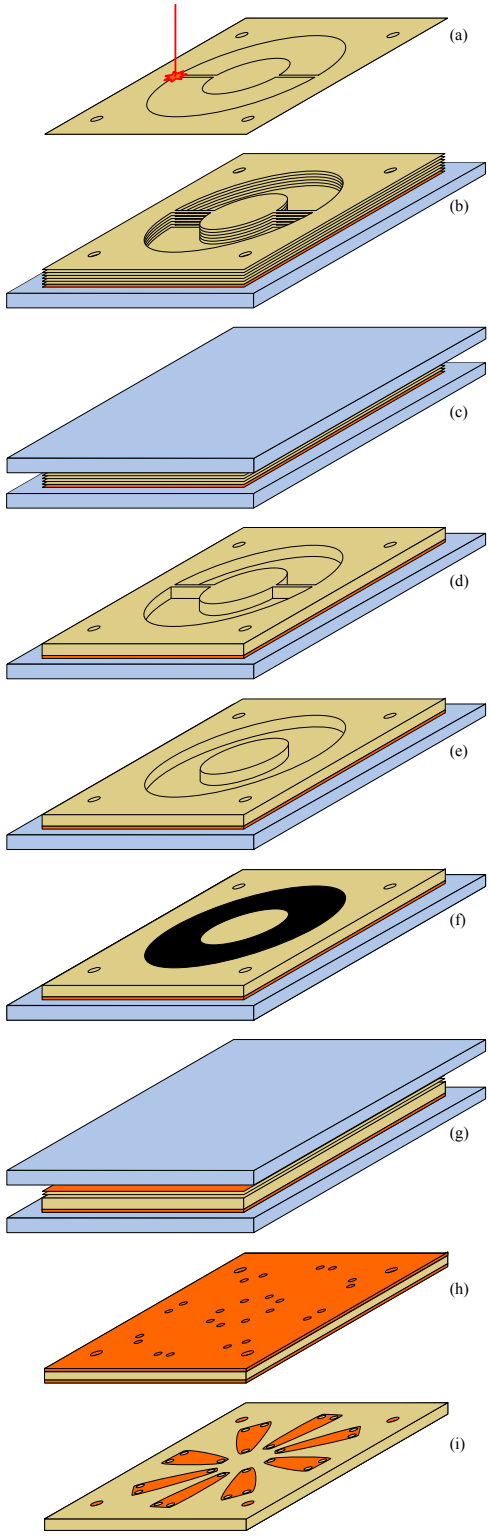

Figure 2: Fabrication of the magnetic component

pliance is to use thinner magnetic layers. In [8], the authors use thin (20 μm) sheets of amorphous material, to embed a 30 W flyback transformer in a 1 mm thick PCB. Two copper layers and vias are used to form the windings. However, this magnetic material requires an electrical insulation of each layer, and may not be suited to higher thickness/power. This is also true for the work described in [9], which uses a different structure. Here, the windings are built using a single (internal) copper layer, surrounded by two thin permalloy layers. This structure can be used both for PCB and silicon integration, but remains limited to low power due to the thin magnetic layers used.

A second solution to obtain compliant magnetic layers is to mix magnetic particles with polymers. Zhang *et al.* [10] built inductors using sheets of magnetic flakes in a polymer matrix. Waffenschmidt *et al.* [11] proposed a converter based on "Maglam" (Isola) sheets (ferrite powder in polymer), with a relative permeability of 17. An alternative method is to apply the magnetic particles/polymer mixture and to cure it in place. This method was introduced in [12], using polyimide as the matrix. Its application to manufacturing PCB inductor is presented in [13].

In this paper, we present an alternative approach to form magnetic components. To create the magnetic core, a cavity is formed in a printed circuit board prior to its lamination. This cavity is filled with ferrite powder (without any binder or matrix). The PCB is then laminated, encapsulating the ferrite powder, and windings are formed by patterning the copper layers.

The manufacturing process is detailed in the next section. The results are given in section 3, and discussed in section 4.

2 Embedding of powder materials

The approach developed in this paper is summarised in Fig. 1: a "mould" is formed by stacking some stage-B epoxy-glass composite sheets ("prepregs"). This mould is filled with ferrite powder. Then, a curing cycle is performed to cure the resin and form a solid part. A mechanical pressure is applied to ensure good bonding, reduce the air gaps between the ferrite particles, and force the resin to infiltrate the ferrite.

The reference of the ferrite material used in this paper is FMS 0.250 (Ferroxcube [3], 71% Fe_2O_3, 20.7% MnO, 8.3% Zn0). It is supplied as a powder, with the following particle size distribution: d10 $= 8-10$ μm, d50 $= 80-120$ μm, d90 $= 250-300$ μm. This material is intended for cable shielding, so its exact composition may vary, and no actual permeability value is quoted. It was selected because it was readily available in powder form. A more detailed description of the embedding process is presented in Fig. 2.

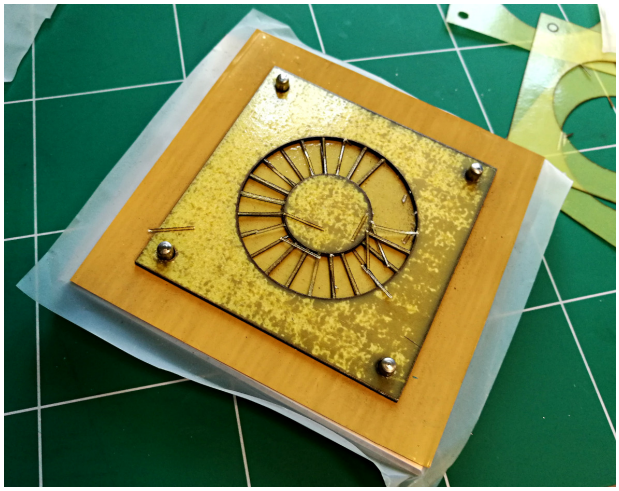

Figure 3: Photograph of the stack between stages (d) and (e) in Fig. 2: the small bridges which maintained the centre of the mould are being removed. In this photograph, many bridges are visible because they are offset from one prepreg layer from the next (there are actually 4 bridges per layer). The external diameter of the cavity is 50 mm.

As it can be seen, this process is fairly straightforward. The main difference with standard PCB process is that it only uses prepreg sheets to form the final laminate instead of a mix of pre-cured boards and prepreg sheets. This requires much more layers (in our case, more than 20 prepreg sheets are formed to achieve a final height of 1.4 mm). Another difference is the step (c) in Fig. 2, where the prepreg sheets are forced together at low temperature. This ensure there is no gap between the prepreg sheets where the ferrite particles could penetrate. Note that the removing of the bridges (Fig. 2(e)) could be automated using a standard CNC router instead of a sharp knife.

Two annular inductor designs were built: a "large" one (external diameter 50, internal diameter 25 mm) and a "small" one (external diameter 19 mm, internal diameter 6 mm). 20 Prepreg sheets were stacked to form the cavity, resulting in an estimated thickness for the magnetic core of 1.27 mm (each 1080 prepreg sheet has a laminated thickness of 64.5 μm (2 mils).

3 Electrical characterisation

An example of electrical measurements performed on the "small" tore design are presented in Fig. 5. The equivalent permeability of the core can be calculated using:

$$L = \frac{\mu_0 \mu_r N^2 A}{\pi d} \tag{1}$$

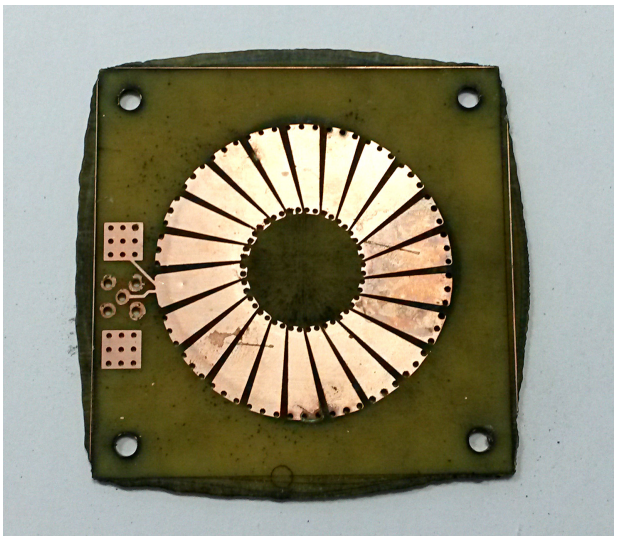

Figure 4: Photograph of an inductor built using the process described in section 2

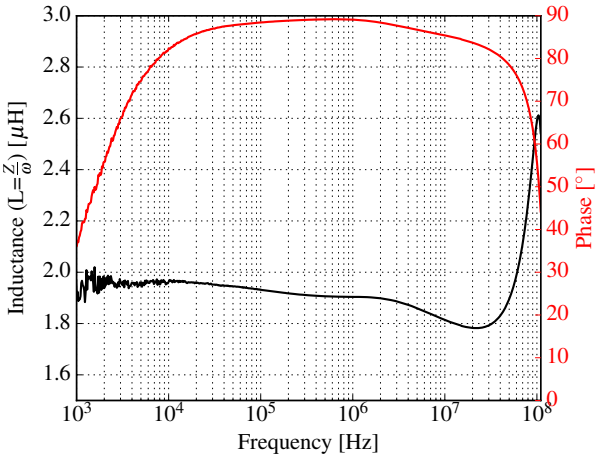

Figure 5: Inductance / Phase plot of a "small" inductor (OD 19 mm, ID 6 mm) with 16 turns, measured with a Keysight E4990 impedance analyser.

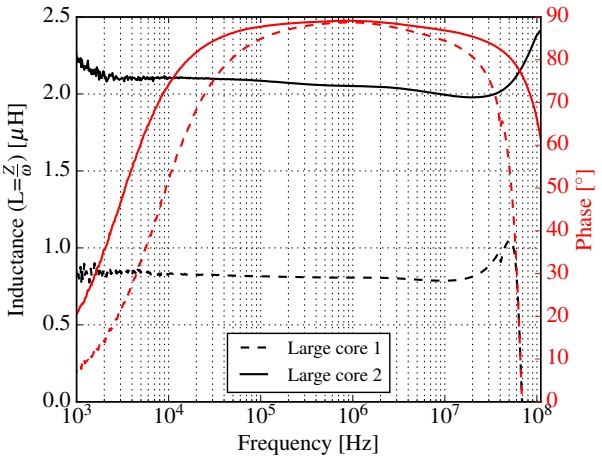

Figure 6: Inductance / Phase plot of two "large" inductors (OD 50 mm, ID 35 mm) with 22 turns.

With L the inductance value (1.9 μH, as visible in Fig. 5), μ_0 the vacuum permeability (1.2566×10^{-6}m.kg.s^{-2}.A^{-2}), μ_r the relative permeability, N the number of turns of the winding (here 16), A the section area (8.26 mm^2) and d the average diameter (12.5 mm). Using eq. (1), μ_r is found to be 28.

For the large tore (Fig. 6), two inductors were assembled, and resulted in very different inductance values (0.8 and 2.1 μH). Considering N=22, A=17 mm^2, d=37.5 mm, μ_r is found to be 9 and 24 for L=0.8 μH and 2.1 mH respectively. This indicates that the ferrite density was different for both cores, resulting in larger distributed airgaps for the core with the smallest inductance value.

A B(H) curve, measured on the small core at 100 Hz, is presented in Fig. 7. The amplitude of the curve was limited by our measurement setup, so we could not observe the saturation of the magnetic material (expected to be around 0.4 T for MnZn ferrite materials from Ferroxcube).

4 Discussion

Although the permeability of ferrite material used here is unknown (it is not quoted in the Ferroxcube datasheet [3] as this material is dedicated to cable shielding, not to power conversion), it is expected to be anywhere between a few hundred and a few thousand. therefore, the measured equivalent permeabilities (9 to 28) indicate that the produced cores have large distributed air gaps. Another consequence of these air-gaps is the "graceful saturation", a desirable feature in power electronics whose onset is visible in Fig. 7.

Assuming that the permeability of the ferrite is much larger than μ_0, one can estimate that the equivalent permeability of the core is $\mu_r = l/g$ with l the average length of the core ($l = \pi d$), and g the total length of the air gap. For the small core ($\mu_r = 28$), this corresponds to $g = 1.4$ mm. For the large core with $\mu_r = 24$, $g = 4.9$ mm. For this core, the weight of ferrite material incorporated is 5.5 g for a cavity volume of 1.635 cm^3. This corresponds to a density of 3.36 g/cm^3, consistent with the "tap density" quoted in [3]. For the large core with $\mu_r = 9$, $g = 13$ *mm*, indicating that the density of the ferrite particles is probably much lower.

Both acceptable cores (the small core and the large core with $\mu_r = 24$) were cut and polished. Scanning Electron Microscope images of these cross-sections are visible in Fig. 8. In Fig. 8a, it can be seen that there is a clear limit

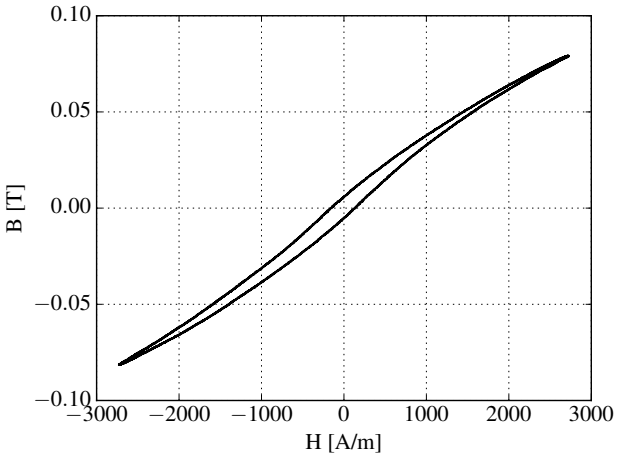

Figure 7: B(H) curve measured for the small core at 100Hz.

between the PCB laminate (left side of the picture) and the ferrite area, which indicates that the prepreg sheets were well bonded during the low temperature pressing stage (Fig. 2(c)). The size distribution of the ferrite particles is consistent with the datasheet of the powder [3], with large particles of up to 500 μm in size, and a large quantity of much smaller particles. The spatial distribution, however, is not uniform, with most of the small particles on top in Fig. 8a. This might be a consequence of the tapping (step (f) in Fig. 2). All the space between the particles appear to be filled with resin.

For the large core (and for other areas of the small core, not shown here), the resin did not penetrate as deeply (Fig. 8b). Most of the cavity remained free from resin, and the ferrite particles fell off during the preparation of the micro-section. This poor penetration of the resin could be either be caused to trapped air (our laminating press does not allow lamination under vacuum), or to the resin flowing mainly out of the prepreg stack. The volume of resin which flowed out of the stack (this corresponds to the areas outside of the external square in Fig. 4) is approximately equal to the volume of resin in the prepregs prior to lamination. This indicates that little resin flowed inwards.

Overall, the permeability of these ferrite powder cores is relatively low compared to that of solid cores. However, it compares favourably with that of other "ferrite in polymer" solutions ($\mu_r = 17$ in [11], 7.2 in [13]).

Although well suited to small-scale testing, this method may be difficult to scale-up because it relies on a fairly large stack of prepreg sheets, and because of the difficulty in handling properly the magnetic powder (powder residues over the board). This latter issue might be addressed by a more controlled granulometry of the powder (to remove the smallest particles), and by the addition of a binder –liquid epoxy resin– to form a paste which might be easier to dispense in the cavities.

5 Conclusion and Perspectives

We presented a method suitable for the embedding of magnetic cores in a printed circuit board. This methods allows does not present major limitations in terms of core size or shape (providing they fit within the PCB). It relies on the resin flow which occurs during lamination of the PCB to bind the ferrite particles, and on the lamination pressure to increase the powder density. Demonstrators (inductors) made using a MnZn ferrite material show relative permeability values of up to 28.

Large variations in permeability values were found, indicating a variation in the ferrite powder density between inductors. A better control of the cavity filling might be required to improve reproducibility (for example by measuring the weight of ferrite powder). Also, it was found that in some cases, the resin did not infiltrate uniformly between the ferrite particles. Further investigations are required to refine the lamination parameters and achieve better infiltration.

6 Acknowledgement

The authors thank the 3DPHI national platform for giving access to their equipment and Mr Gilles BRILLAT and his team (Univ. Paul SABATIER, Toulouse) for their technical assistance.

References

[1] A. Alderman, L. Burgyan, B. Narveson, and E. Parker, "3-D Embedded Packaging Technology," *IEEE Power Electronics Magazine*, pp. 30–39, dec 2015.

[2] A. Ostmann, "Evolution and future of embedding technology," in *IMAPS/NMI workshop "disappearing die – embed your chips"*, 2016.

[3] Ferroxcube, "Fms material specification – fxc milled ferrite cores," Ferroxcube, Tech. Rep., 2013.

[4] Q. Chen, Z. Gong, X. Yang, Z. Wang, and L. Zhang, "Design considerations for passive substrate with ferrite materials embedded in printed circuit board (pcb)," in *2007 IEEE Power Electronics Specialists Conference*, June 2007, pp. 1043–1047.

[5] M. Ali, E. Labouré, F. Costa, and B. Revol, "Design of a hybrid integrated emc filter for a dc–dc power converter," *IEEE Transactions on Power Electronics*, vol. 27, no. 11, pp. 4380–4390, 2012.

[6] B. Sun, R. Burgos, D. Boroyevich, R. Perrin, C. Buttay, B. Allard, N. Quentin, and M. Ali, "Two Comparison-Alternative High Temperature PCB-Embedded Transformer Designs for a 2 W Gate

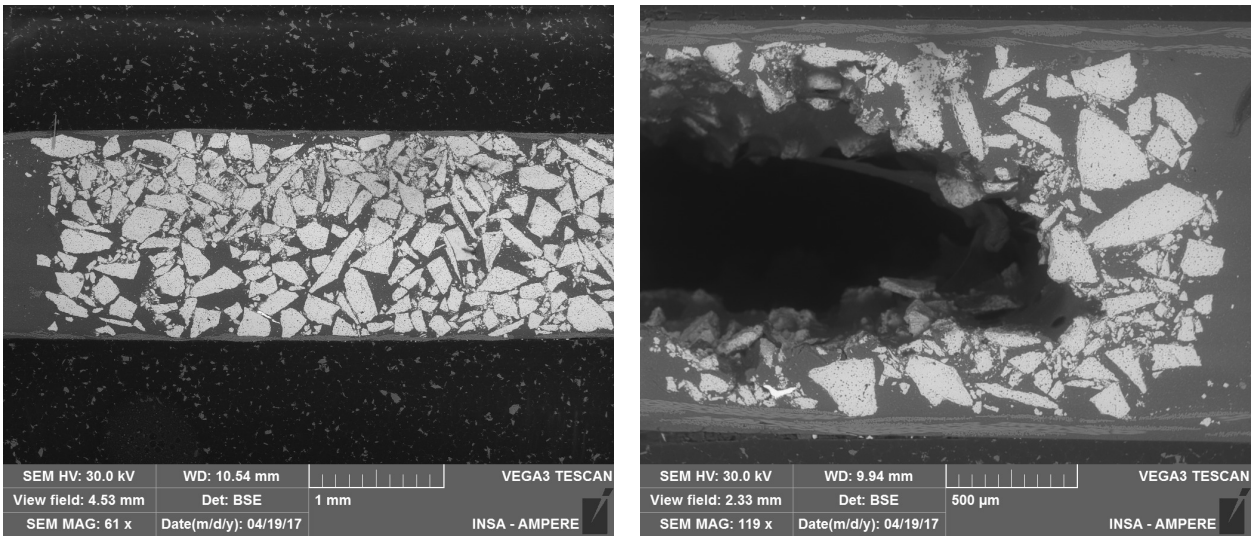

(a) (b)

Figure 8: Micro-sections on a "small" core (a) and on a "large" core (b). For the small core, the resin infiltrated between most of the ferrite particle (there are some voids, not shown here), but for the large core, only part of the ferrite particles were bonded by the prepreg resin. The rest of the ferrite particles were not bonded and fell during the preparation of the cross section.

Driver Power Supply," in *IEEE Energy Conversion Congress and Expo (ECCE 2016)*. Milwaukee, WI, United States: IEEE, Sep. 2016. [Online]. Available: https://hal.archives-ouvertes.fr/hal-01373036

[7] R. Perrin, B. Allard, C. Buttay, N. Quentin, W. Zhang, R. Burgos, D. Boroyevich, P. Preciat, and D. Martineau, "2 MHz high-density integrated power supply for gate driver in high-temperature applications," in *Applied Power Electronics Conference and Exposition (APEC)*, Long Beach, United States, Mar. 2016. [Online]. Available: https://hal.archives-ouvertes.fr/hal-01372141

[8] C. Marxgut, J. Muhlethaler, F. Krismer, and J. W. Kolar, "Multiobjective optimization of ultraflat magnetic components with pcb-integrated core," *IEEE Transactions on Power Electronics*, vol. 28, no. 7, pp. 3591–3602, 2013.

[9] S. C. Ó Mathúna, P. Byrne, G. Duffy, W. Chen, M. Ludwig, T. O' Donnel, P. McCloskey, and M. Duffy, "Packaging and integration technologies for future high-frequency power supplies," *IEEE transactions on industrial Electronics*, vol. 51, no. 6, pp. 1305 – 1312, 2004.

[10] W. Zhang, Y. Su, M. Mu, D. J. Gilham, Q. Li, and F. C. Lee, "High-density integration of high-frequency high-current point-of-load (pol) modules with planar inductors," vol. 30, no. 3, pp. 1421–1431, Mar. 2015.

[11] E. Waffenschmidt, B. Ackermann, and J. A. Ferreira, "Design Method and Material Technologies for Passives in Printed Circuit Board Embedded Circuits," *IEEE Transactions on Power Electronics*, vol. 20, no. 3, pp. 576–584, May 2005.

[12] J. Y. Park and M. G. Allen, "Low temperature fabrication and characterization of integrated packaging-compatible, ferrite-core magnetic devices," in *Applied Power Electronics Conference and Exposition (APEC) Conference Proceedings*, 1997.

[13] D. H. Bang and J. Y. Park, "Ni-zn ferrite screen printed power inductors for compact dc-dc power converter applications," *IEEE Transactions on Magnetics*, vol. 45, no. 6, pp. 2762–2765, June 2009.